**Hydrology and
Earth System
Sciences**

Water balance modeling of Upper Blue Nile catchments using a top-down approach

S. Tekleab[1,2,3,4], **S. Uhlenbrook**[1,4], **Y. Mohamed**[1,4], **H. H. G. Savenije**[4], **M. Temesgen**[1,5], and **J. Wenninger**[1,4]

[1]UNESCO-IHE Institute for Water Education, P.O. Box 3015, 2601 DA Delft, The Netherlands
[2]Addis Ababa University, Institute for Environment, Water and Development, Addis Ababa University, P.O. Box 1176, Addis Ababa, Ethiopia
[3]Hawassa University, Department of Irrigation and Water Resources Engineering, P.O. Box 5, Hawassa, Ethiopia
[4]Delft University of Technology, Faculty of Civil Engineering and Applied Geosciences, Water Resources section, Stevinweg 1, P.O. Box 5048, 2600 GA Delft, The Netherlands
[5]Addis Ababa University, Department of Civil Engineering, P.O. Box 385, Addis Ababa, Ethiopia

Abstract. The water balances of twenty catchments in the Upper Blue Nile basin have been analyzed using a top-down modeling approach based on Budyko's hypotheses. The objective of this study is to obtain better understanding of water balance dynamics of upper Blue Nile catchments on annual and monthly time scales and on a spatial scale of meso scale to large scale. The water balance analysis using a Budyko-type curve at annual scale reveals that the aridity index does not exert a first order control in most of the catchments. This implies the need to increase model complexity to monthly time scale to include the effects of seasonal soil moisture dynamics. The dynamic water balance model used in this study predicts the direct runoff and other processes based on the limit concept; i.e. for dry environments since rainfall amount is small, the aridity index approaches to infinity or equivalently evaporation approaches rainfall and for wet environments where the rainfall amount is large, the aridity index approaches to zero and actual evaporation approaches the potential evaporation. The uncertainty of model parameters has been assessed using the GLUE (Generalized Likelihood Uncertainty Estimation) methodology. The results show that the majority of the parameters are reasonably well identifiable. However, the baseflow recession constant was poorly identifiable. Parameter uncertainty and model structural errors could be the reason for the poorly identifiable parameter. Moreover, a multi-objective model calibration strategy has been employed to emphasize the different aspects of the hydrographs on low and high flows.

The model has been calibrated and validated against observed streamflow time series and it shows good performance for the twenty study catchments in the upper Blue Nile. During the calibration period (1995–2000) the Nash and Sutcliffe efficiency (E_{NS}) for monthly flow prediction varied between 0.52 to 0.93 (dominated by high flows), while it varied between 0.32 to 0.90 using logarithms of flow series (indicating the goodness of low flow simulations). The model is parsimonious and it is suggested that the calibrated parameters could be used after some more regionalization efforts to predict monthly stream flows in ungauged catchments of the Upper Blue Nile basin, which is the vast majority of catchments in that region.

1 Introduction

The Blue Nile river emanates from Lake Tana in Ethiopia at an elevation of 1780 m a.s.l. Approximately 30 km downstream of Lake Tana, at the Blue Nile falls, the river falls in to a deep gorge and travels about 940 km till the Ethiopian-Sudanese boarder (Conway, 1997). Despite its 60 % of annual flow contribution to the Nile river (e.g. UNESCO, 2004; Conway, 2005), the research in the Blue basin has suffered from limited hydrological and climatic data availability, which hampers an in-depth study of the hydrology of the basin.

The hydrology of the Upper Blue Nile basin was studied using a simple water balance model (e.g. Johnson and Curtis, 1994; Conway, 1997; Mishra and Hata, 2006; Steenhuis et al., 2009). However, most of these studies were conducted on large scale to analyze the flow at the outlet at the

Ethiopian-Sudanese border. An understanding of the processes at sub-catchment level is generally lacking. Moreover, as a part of model uncertainty and parameter identifiability studies, multi-objective calibration searching for optimal parameter sets towards different objective functions was missing in previous studies. Another limitation is that most of the hydrological studies in the Blue Nile have been conducted in the Lake Tana sub-basin. For example, the applications of the SWAT model in Lake Tana sub-basins (Setegne et al., 2008, 2010). Kebede et al. (2006) studied the water balance of Lake Tana and its sensitivity to fluctuations in rainfall. Wale et al. (2009) applied HBV model in the Lake Tana sub basin to study ungauded catchment contributions to the Lake Water balance.

Uhlenbrook et al. (2010) studied the hydrological dynamics and processes of Gilgel Abay and Koga catchments using also the HBV model. Assessments of climate change impacts on hydrology of the Gilgel Abay catchment also indicate that the catchment is sensitive to climate change especially to changes in rainfall (Abdo et al., 2009). Gebreyohannis et al. (2010) studied the relation of forest cover and streamflow in the headwater Koga catchment through satellite imagery and community perception. They reported that the effect of deforestation for the past four decades did not show any significant change in the flow regime.

Assessment of catchment water balance is a pre-requisite to understand the key processes of the hydrologic cycle. However, the challenge is more distinct in developing countries, where data on climate and runoff is scarce as in the case of Upper Blue Nile basin. In such cases, a water balance study can provide insights into the hydrological behavior of a catchment and can be used to identify changes in main hydrological processes (Zhang et al., 1999). In order to analyze the catchment water balance Budyko (1974) developed a framework linking climate to evaporation and runoff from a catchment. He developed an empirical relationship between the ratio of mean annual actual evaporation to mean annual rainfall and mean annual dryness index of the catchment.

The Budyko hypothesis has been widely applied in the catchments of the former Union of Soviet Socialist Republics (USSR). Similar studies were conducted worldwide using Budyko's framework (e.g. Milly, 1994; Koster and Suarez, 1999; Sankarasubramania and Vogel, 2002, 2003; Zhang et al., 2004; Potter et al., 2005; Donohue et al., 2007; Gerrits et al., 2009; Potter and Zhang, 2009; Yang et al., 2009). All these studies improved Budyko framework by including additional processes. Zhang et al. (2001, 2008) and Yang et al. (2007) suggested that by assuming negligible storage effects for long term mean (>5 year) the annual aridity index ($\Phi = E_0/P$) controls partitioning of precipitation (P) to evaporation (E) and runoff (Q). E_0 is the potential evaporation, while E is actual evaporation. By evaporation we mean all forms of water changes from liquid to vapor, i.e. soil and open water evaporation plus transpiration and interception evaporation. This is often termed evapotranspiration or

total evaporation in the literature. However, Sankarasubramania and Vogel (2002, 2003) argued that the aridity index is not the only variable controlling the water balance at annual time scale and that the evaporation ratio (E/P) is related to soil moisture storage as well. Their results improved by including a soil moisture storage index, which could be derived from the "abcd" watershed model. The abcd watershed model is a nonlinear water balance model which uses precipitation and potential evaporation as input, producing streamflow as output.

The model has four parameters a, b, c and d. The parameter "a" represents the tendency of runoff to occur before the soil is fully saturated. The parameter "b" is an upper limit on the sum of evaporation and soil moisture storage. The parameter "c" represents the fraction of streamflow which, arises from groundwater. The parameter "d" represents the base flow recession constant (Sankarasubramania and Vogel; 2002). Besides, they classified catchments in the US based on the aridity index range of 0–0.33 as humid, 0.33–1 as semi-humid, 1–2 as temperate, 2–3 as semi-arid and 3–7 as arid. Milly (1994) showed that the spatial distribution of soil moisture holding capacity and temporal pattern of rainfall can affect catchment evaporation, but could be of small influence on annual time scale. Obviously, spatial and temporal variability of vegetation affects evaporation and hence the water balance. Thus, it is more important to include the soil moisture storage for smaller spatial and temporal scales (Donohue et al., 2007). Zhang et al. (2004) hypothesized that the plant available water capacity coefficient reflects the effect of vegetation on the water balance. They developed a two parameter model which relates the mean annual evaporation to rainfall, potential evaporation and plant available water capacity to quantify the effect of long term vegetation change on mean annual evaporation ($\overline{E}$) in 250 catchments worldwide and found encouraging results. Inspired by the work of Fu (1981), Yang et al. (2007) analyzed the spatio-temporal variability of annual evaporation and runoff for 108 arid/semi-arid catchments in China and explored both regional and inter-annual variability in annual water balance and confirmed that the Fu (1981) equation can provide a full picture of the evaporation mechanism at the annual timescale.

The distinct feature of the present study as compared to the previous study is that, we learned from the data starts with simple annual model in different sub-catchments with in the Upper Blue Nile basin based on Budyko framework and model complexity is increased to monthly time scale. The monthly water balance model developed by Zhang et al. (2008), which is based on the Budyko hypotheses, has been tested in 250 catchments in Australia with different rainfall regimes across various geographical region and they obtained encouraging results. We have applied this model in the Upper Blue Nile catchments due to its parsimony, only having four physically meaningful parameters and its versatility to predict streamflow and to investigate impacts of

vegetation cover change on stream flow. Fang et al. (2009) applied the model in Australian and South African catchments on a monthly time scale and meso-scale and to large scale to study land cover change impacts on streamflow.

Moreover, in data scares environment like the Upper Blue Nile basin, complex models which require more input data and large number of parameters are not recommended. The model used in this study has only four parameters. The most commonly used hydrological models which have been applied in the Blue Nile basin are conceptual semi-distributed model like the Soil and Water Assessment Tool (SWAT) (more than 20 parameters, many temporal variable) and the conceptual HBV model (Hydrologiska Byråns Vattenbalansavdelning) has (12 parameters). They have many more parameters than the four parameters model used in this study. Therefore, in terms of over parameterization, which is the major cause of equifinality, the previous models were more prone to equifinality problem than the model we used in this study.

The objective of this paper is building on the work of Budyko (1974), Fu (1981), Zhang et al. (2004, 2008) to investigate the water balance dynamics of twenty catchments in the Upper Blue Nile on temporal scales of monthly and annual and spatial scales of meso-scale (catchment area between 10–1000 km^2) to large scale (catchment area > 10 000 km^2). Consequently, the basis for predicting water balance parameters in ungauged basins is laid.

2 Study area and input data

2.1 Study area

The Upper Blue Nile River is located in the highlands of Ethiopia (Fig. 1). The elevation ranges between 489 on the western side to 4261 m a.s.l. at Mount Ras Dashen in the north-eastern part. The catchment boundary and the drainage pattern have been delineated using ArcGIS 9.3 with a 90 m resolution digital elevation model of the NASA Shuttle Radar Topographic Mission (SRTM) obtained from the Consortium for Spatial Information (CGIR_CSI) website (http://srtm.csi.cgiar.org).

The climate in the Upper Blue Nile river basin varies from humid to semi-arid and it is mainly dominated by latitude and altitude. The influence of these factors determine a rich variety of local climates, ranging from hot and arid along the Ethiopia-Sudan border to temperate at the highlands and even humid-cold at the mountain peaks in Ethiopia. According to the present study, the mean annual temperature ranges from 13 °C in south eastern parts to 26 °C in the lower areas of the south western part for the period 1995–2004. The Ethiopian National Meteorological Services Agency (ENMA) defines three seasons in Ethiopia: rainy season (June to September), dry season (October to January) and short rainy season (February to May). The

short rains, originating from the Indian Ocean, are brought by south-east winds, while the heavy rains in the wet season originate mainly from the Atlantic Ocean and are related to south-west winds (BCEOM, 1999; Seleshi and Zanke, 2004). The study by Camberlin (1997) reported that the monsoon activity in India is a major cause for summer rainfall variability in the East African highlands. A recent study by Haile et al. (2009) showed that the variation of rainfall at the source of the Blue Nile River in Lake Tana sub-basin is affected by terrain elevation and distance to the center of the Lake. Moreover, in their study it is indicated that the amount of nocturnal rainfall (rainfall during the night time) over the Lake shore was about 75 % of the total rainfall and it is higher than the nocturnal rainfall over the mountainous areas.

The rainfall in the basin has a mono-modal pattern. Annual rainfall values constructed from eleven gauges range between 1148–1757 mm yr^{-1} during the period 1900–1998 has a mean value of 1421 mm yr^{-1} and 70 % of it concentrates between June and September (Conway, 2000). Abtew et al. (2009) studied the spatial and temporal distribution of meteorological parameters in the upper Blue Nile basin. According to their study the mean annual rainfall is 1423 mm yr^{-1} for the period of 1960–1990. The dominant land cover in the basin is rainfed agriculture, i.e. cropland (26 %) and grassland (25 %). Wood and shrub land are minor compared to the other land cover types (Teferi et al., 2010). The soil type in the basin is dominated by Vertisol and Nitisol types (53 %). The Nitisols are deep non swelling clay soils with favorable physical properties like drainage, workability and structure, while the Vertisols are characterized by swelling clay minerals with more unfavorable conditions. The basin geology is characterized by basalt rocks, which are found in the Ethiopian highlands, while the lowlands mainly composed of basement rocks and metamorphic rocks such as gneisses and marbles (ENTRO, 2007).

2.2 Input data

Monthly stream flow time series of 20 rivers covering the period 1995–2004 have been collected from the Ministry of Water Resources Ethiopia, Department of Hydrology. The quality of the input data has been checked based on comparison graphs of neighboring stations and also double mass analyses were carried out to check the consistency of the time series on a monthly basis. The missing data were filled in using regression analysis. Monthly meteorological data for the same period were obtained from the Ethiopian National Meteorological Agency (ENMA). The data comprises precipitation from 48 stations and temperature from 38 stations. Potential evaporation was computed using Hargreaves method with minimum and maximum average monthly temperature as input data (Hargreaves and Samani, 1982). This method was selected due to the fact that meteorological data in the region is scarce, which limits the possibility to use different methods for the computation of potential evaporation.
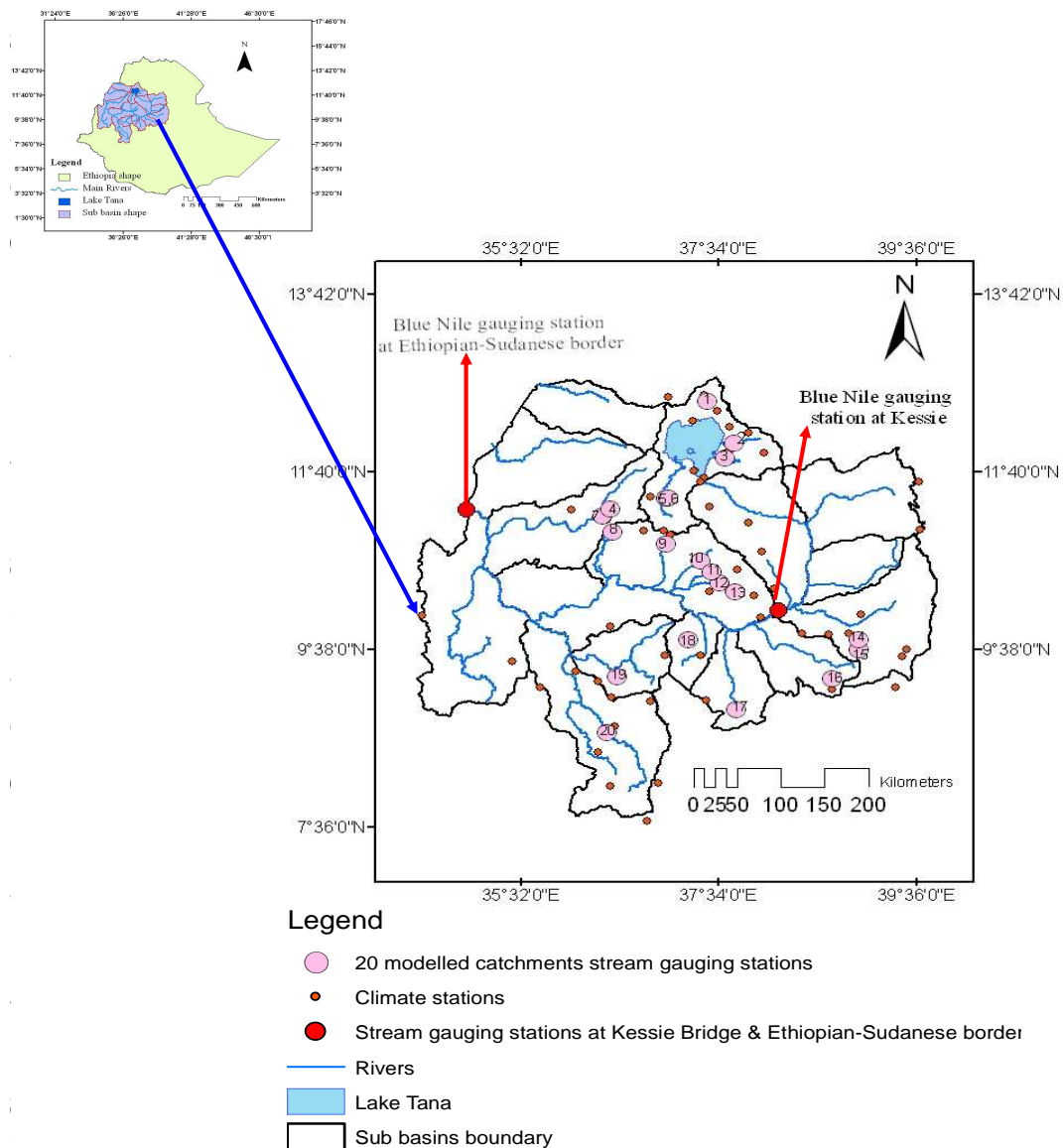
Fig. 1. Study area; numbers indicate the location of gauging stations of modeled catchments.

However, the Penman-Monteith method, which has been applied successfully in different parts of the world, was compared with other methods and is accepted as the preferred method for computing potential evaporation from meteorological data (Allen et al., 1998; Zhao et al., 2005). The Hargreaves model was recommended for the computation of potential evaporation, if only the maximum and minimum air temperatures are available (Allen et al., 1998). Hargreaves and Allen (2003) also reported that the results computing the monthly potential evaporation estimates obtained using Hargreaves method were satisfactory. For example Sankarasubramania and Vogel (2003) used Hargreaves model to estimate the monthly potential evaporation in 1337 catchments in US. Table 1 presents basic hydro-meteorological characteristics of the twenty study catchments.

3 Methodology

3.1 The Budyko framework

Budyko-type curves were developed by many researchers in the past (Schreiber, 1904; Ol'dekop, 1911; Turc, 1954; Pike, 1964; Fu, 1981). The assumptions inherent to the Budyko framework are:

1. Considering a long period of time ($\tau \geq 5$ years), the storage variation in catchments may be disregarded (i.e. $\Delta S \approx 0$).

2. Long term annual evaporation from a catchment is determined by rainfall and atmospheric demand. As a result, under very dry conditions, potential evaporation

Table 1. Hydro-meteorological characteristics of the investigated twenty upper Blue Nile catchments (1995–2004); P, E_0, Q and E stand for basin precipitation, potential evaporation, discharge and actual evaporation, respectively.

Catchment number	Catchment name	Area (km^2)	Long term mean annual values (mm yr^{-1})			
			P	E_0	Q	E
1	Megech	511	1138	1683	421	717
2	Rib	1289	1288	1583	349	939
3	Gumera	1269	1330	1671	841	488
4	Beles	3114	1402	1826	643	759
5	Koga	295	1286	1751	606	679
6	Gilgel Abay	1659	1724	1719	1043	681
7	Gilgel Beles	483	1703	1741	897	806
8	Dura	592	2061	1788	1004	1056
9	Fetam	200	2357	1619	1400	956
10	Birr	978	1644	1677	553	1091
11	Temcha	425	1409	1512	623	785
12	Jedeb	277	1449	1454	861	587
13	Chemoga	358	1441	1454	461	980
14	Robigumero	938	1052	1362	289	762
15	Robijida	743	1002	1379	222	780
16	Muger	486	1215	1654	480	735
17	Guder	512	1734	1744	713	1020
18	Neshi	327	1654	1416	686	967
19	Uke	247	1957	1488	1355	602
20	Didessa	9672	1538	1639	334	1204

Fig. 2. Budyko curve representing evaporation ratio is a function of aridity index.

The water balance equation of a catchment at annual time scale can be written as:

$$\frac{\mathrm{d}S}{\mathrm{d}t} = P - Q - E \tag{2}$$

where: P is precipitation (mm yr^{-1}), Q is the total runoff (mm yr^{-1}), i.e. sum of surface runoff, interflow and baseflow, E is actual evaporation (mm yr^{-1}), $\frac{\mathrm{d}S}{\mathrm{d}t}$ is storage change per time step (mm yr^{-1}).

By assuming storage fluctuations are negligible over long time scales, i.e. $\tau \geq 5$ years, Eq. (2) reduces to:

$$P - Q - E = 0 \tag{3}$$

Equation (3) is known as a steady state or equilibrium water balance, which is controlled by available water and atmospheric demand controlled by available energy (Budyko, 1974; Fu, 1981; Zhang et al., 2004, 2008).

Among the different of Budyko-type curves, we used Eq. (4) given by:

$$\frac{E}{P} = 1 + \frac{E_0}{P} - \left[1 + \left(\frac{E_0}{P}\right)^w\right]^{\frac{1}{w}} \tag{4}$$

Details of the derivation of this equation can be found in (Zhang et al., 2004). This equation has one annual parameter w [−], which is a coefficient representing the integrated effects of catchment characteristics such as vegetation cover, soil properties and catchment topography on the water balance (Zhang et al., 2004). This equation would enable to model individual catchments on annual basis. Even though, the results from different Budyko-type curves are not presented here, prediction of annual runoff and evaporation using Eq. (4) was better than the other Budyko-type curves. The selection of Eq. (4) was based on the Nash and Sutcliffe efficiency criterion/measure. Moreover, most of Budyko-type curves including Budyko (1974) do not have calibrated parameters and could not be applied on individual catchments (Potter and Zhang, 2009).

may exceed precipitation, and actual evaporation approaches precipitation. These relations can be written as $\frac{Q}{P} \to 0$, $\frac{E}{P} \to 1$, and $\frac{E_0}{P} \to \infty$. Similarly, under very wet conditions, precipitation exceeds potential evaporation, and actual evaporation asymptotically approaches the potential evaporation $E \to E_0$, and $\frac{E_0}{P} \to 0$.

The Budyko (1974) equation can be written as:

$$\frac{E}{P} = \left[\phi \tanh\left(\frac{1}{\phi}\right)\left(1 - \exp^{-\phi}\right)\right]^{0.5} \tag{1}$$

The Budyko curve representing the energy and water limit asymptotes are shown in Fig. 2.

3.2 Catchment water balance model at annual time scale

To study catchment water balance hydro-meteorological variables have been prepared for the model as an input. The average precipitation and potential evaporation for each twenty catchments have been estimated using thiesen polygon method. Figure 1 illustrates the hydro-meteorological location used in this study. Due to scares data availability with many gaps in the time series, only twenty catchments with relatively having good quality of streamflow, precipitation and temperature measurements were used in this study.

The two performance measures Nash and Sutcliffe co-efficient of efficiency (E_{NS}) and root mean squared error (RMSE) were used in the annual model, and are defined as follows:

$$E_{\mathrm{NS}} = (1) - \frac{\sum\limits_{i=1}^{n} \left(Q_{\mathrm{sim},i} - Q_{\mathrm{obs},i}\right)^2}{\sum\limits_{i=1}^{n} \left(Q_{\mathrm{obs},i} - \overline{Q}_{\mathrm{obs},i}\right)^2} \quad (5)$$

$$\mathrm{RMSE} = \sqrt{1/n \cdot \sum_{i=1}^{n} \left(Q_{\mathrm{obs},i} - Q_{\mathrm{sim},i}\right)^2} \quad (6)$$

where $Q_{\mathrm{sim},i}$ is the simulated streamflow at time i [mm yr^{-1}], $Q_{\mathrm{obs},i}$ is the observed streamflow at time i [mm yr^{-1}], n is the number of time steps in the calibration period and the over-bar indicates the mean of observed streamflow.

3.3 Catchment water balance model at monthly time scale

The dynamic water balance model developed by Zhang et al. (2008) has been used to simulate the monthly streamflow. The model has four parameters describing direct runoff behavior α_1 [−], evaporation efficiency α_2 [−], catchment storage capacity S_{max} [mm], and slow flow component d [1/month]. Zhang et al. (2008) stated that each parameter can be interpreted physically. For example the parameter α_1 represents catchment rainfall retention efficiency and an increase in parameter α_1 implies higher rainfall retention and less direct runoff. The maximum soil water storage in the root zone (S_{max}) relates to soil and vegetation characteristics of the catchment. The parameter α_2 relates to the evaporation efficiency, a

higher value implies a higher partitioning of available water to evaporation. The parameter d represents the baseflow and groundwater storage behavior. The model uses rainfall and potential evaporation data as an input to simulate monthly streamflow. A schematic diagram for the dynamic water balance model is shown in Fig. 3.

Details of the equations in Fig. 3 and model descriptions are presented in the Appendix. This dynamic conceptual monthly water balance model has two storages: the root zone storage and groundwater storage and both act as linear storage reservoirs. State variables and fluxes are defined based in Eq. (4). Referring to Eq. (4), w [−] is a model parameter ranging between 1 and ∞. For the purpose of model calibration Zhang et al. (2008) defined that $\alpha = 1 - \frac{1}{w}$, this implies that α [−] values vary between 0 and 1.
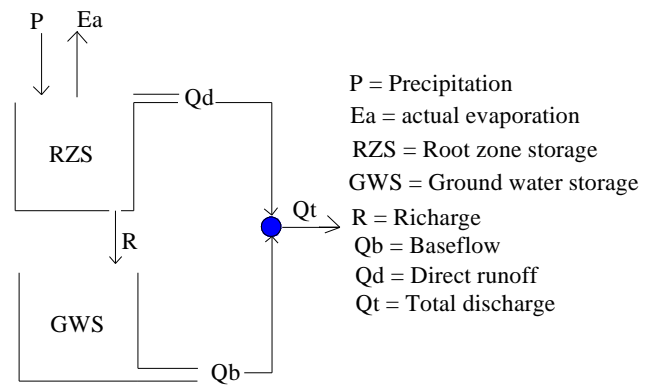
Fig. 3. Schematic diagram of monthly water balance model structure; the unit of all variables for fluxes (P, E_{a}, Q_{d}, Q_{b} and Q_{t}) is mm month^{-1} and mm for the storage parameters (RZS and GWS).

P = Precipitation
Ea = actual evaporation
RZS = Root zone storage
GWS = Ground water storage
R = Recharge
Qb = Baseflow
Qd = Direct runoff
Qt = Total discharge

3.4 Parameter estimation, sensitivity and uncertainty assessment

In this study both manual and automatic calibration procedures have been done to estimate the best parameters set. All twenty catchments and the larger catchments of the Blue Nile at Kessie Bridge station and the Ethiopian-Sudanese border were calibrated on data from 1995–2000, and validated with data sets from 2001–2004 using split sample tests. For the manual calibration and validation, we used the EXCEL spreadsheet model developed by Zhang et al. (2008). However, in order to attain the optimal parameter set in the parameter space and to avoid the subjectivity of choosing parameters manually as well as for the parameter uncertainty assessment, we changed the EXCEL spreadsheet model into a MATLAB code. During the automatic calibration the Generalized Likelihood Uncertainty Estimation framework (GLUE) by Beven and Binley (1992) was employed to constrain model parameters using the Nash and Sutcliffe efficiency as likelihood measure. A threshold value of 0.7 for all catchments has been considered for behavioral models. Monte Carlo simulations employing 20 000 randomly parameter sets have been used to constrain the parameters in a feasible parameter space. Since the E_{NS} was not improved beyond 20 000 simulations and the parameter uncertainty did not change for more simulations, the number of 20 000 simulations has been considered as sufficient for all catchments to constrain the parameters in the given parameters space. This is reasonable as was shown that the parameter space of much more complex models (e.g. a HBV model with 12 parameters) can be sampled sufficiently with "only" 400 000 model runs (Uhlenbrook et al., 1999).

For the monthly model, we also considered a multi-objective optimization using two objective functions directed towards high flows and low flows. In this calibration process, all model parameters were simultaneously calibrated to minimize the objective function towards high flows and low

flows. The concept of Pareto optimality is based on the notion of domination. It is used to solve the multi-objective optimization and derive Pareto-optimal parameter sets (Fenicia et al., 2007). All Pareto-optimal solutions are not dominated by the others. Mapping the Pareto-optimal solutions in a feasible parameter space produce Pareto-optimal front, this consists of more than one solution. Past research pointed out that calibration based on one single objective function often results in unrealistic representation of the hydrological system behavior. This means, the information content of the data is not fully explained in a single objective function (Gupta et al., 1998; Fenicia et al., 2007). In a monthly model the following evaluation criteria were used in this study.

$$F_{\text{HF}} = \frac{\sum\limits_{i=1}^{n} \left(Q_{\text{sim},i} - Q_{\text{obs},i} \right)^2}{\sum\limits_{i=1}^{n} \left(Q_{\text{obs},i} - \overline{Q}_{\text{obs}} \right)^2} \quad (7)$$

$$F_{\text{LF}} = \frac{\sum\limits_{i=1}^{n} \left[\ln \left(Q_{\text{sim},i} \right) - \ln \left(Q_{\text{obs},i} \right) \right]^2}{\sum\limits_{i=1}^{n} \left[\ln \left(Q_{\text{obs},i} \right) - \ln \left(\overline{Q}_{\text{obs}} \right) \right]^2} \quad (8)$$

where $Q_{\text{sim},i}$ [mm month^{-1}] is the simulated streamflow at time i, $Q_{\text{obs},i}$ [mm month^{-1}] is the observed streamflow at time i, n is the number of time steps in the calibration period and the over-bar indicates the mean of observed streamflow. The objective function F_{HF} was selected to minimize the errors during high flows (same formula as E_{NS}), and F_{LF} uses logarithmic values of streamflow and improves the assessment of the low flows.

4 Results and discussions

4.1 Annual water balance

The annual water balance has been computed for the twenty catchments of the Upper Blue Nile basin with the assumption that evaporation can be estimated from water availability and atmospheric demand. Among the different Budyko's type curves, which were reported by Potter and Zhang (2009), Eq. (4) has been applied to compute E/P for the twenty catchments. The selection of this equation was based on the simulation results from each catchment evaluated using Nash and Sutcliffe efficiency criteria. The predicted annual streamflow and evaporation results are given in Table 2. In most of these catchments, Eq. (4) could not predict the annual evaporation and stream flow adequately.

The poor accuracy of the prediction is related to the effect of neglecting soil water storage (assuming dS/d$t = 0$) and other error sources could influence the results as well, e.g. the uncertainty of catchment rainfall and the estimation of potential evaporation, seasonality of rainfall, and

Table 2. Model performance using Eq. (4) for annual runoff and annual evaporation during the period (1995–2004).

Performance measure	Runoff		Evaporation	
	min	max	min	max
E_{NS} [−]	−2.37	0.84	−0.39	0.73
RMSE (mm yr^{-1})	62.50	298.30	68.10	279.40

non-stationary conditions of the catchment itself (e.g. land use/cover change). Furthermore, the year to year variability of rainfall depth could be the reason for the poor performance of the model. However, studying the effects of such factors on model simulation at annual time scale was not the objective of this study and needs further research.

Figure 4 illustrates the application of Eq. (4) to predict the regional long term annual mean water balance (1995–2004) of the twenty catchments.

It can be seen that the aridity index varies from 0.7 to 1.5, and some catchments represent a semi-humid environment, when the aridity index less than 1.0 and others are drier with an aridity index greater than 1.0. Based on the aridity index, the Upper Blue Nile catchments can be classified as semi-arid to semi-humid and temperate.

Considering all twenty catchments, the regional mean annual water balance were adequately predicted by Eq. (4) with a single model parameter ($w = 1.8$) the model gave reasonable good performance with a Nash and Sutcliffe efficiency of (E_{NS}) 0.70 and a root mean squared error of 177 mm yr^{-1}. The results of predicting the regional mean annual water balance using Eq. (4) in this study is in agreement with the research work in different parts of the world (e.g. Yang et al., 2007; Zhang et al., 2008; Potter et al., 2005; Potter and Zhang, 2009).

Furthermore, as it can be seen in Fig. 4 that different groups of catchments follow a unique curve with an independent w [−] value. Thus, the results depicts that catchment evaporation ratio varies from catchment to catchment. Based on evaporation ratio catchments are categorized in to three groups, what suggests that each group has different characteristics. Study by Potter and Zhang (2009) classified catchments in Australia based on rainfall regime as winter dominant, summer dominant, seasonal and non-seasonal catchments. Yang et al. (2007) also classified 108 arid to semi-arid catchments in China based on the patterns which the catchments follow on the Fu curve. Moreover, Zhang et al. (2004) categorized catchments in Australia based on vegetation cover as forested and grass land catchments with a higher parameter w values for forested catchments and lower values of the parameter w for grass covered catchments.

Table 3 presents goodness-of-fit statistics as recommended by Legates and McCabe (1999) for each group of
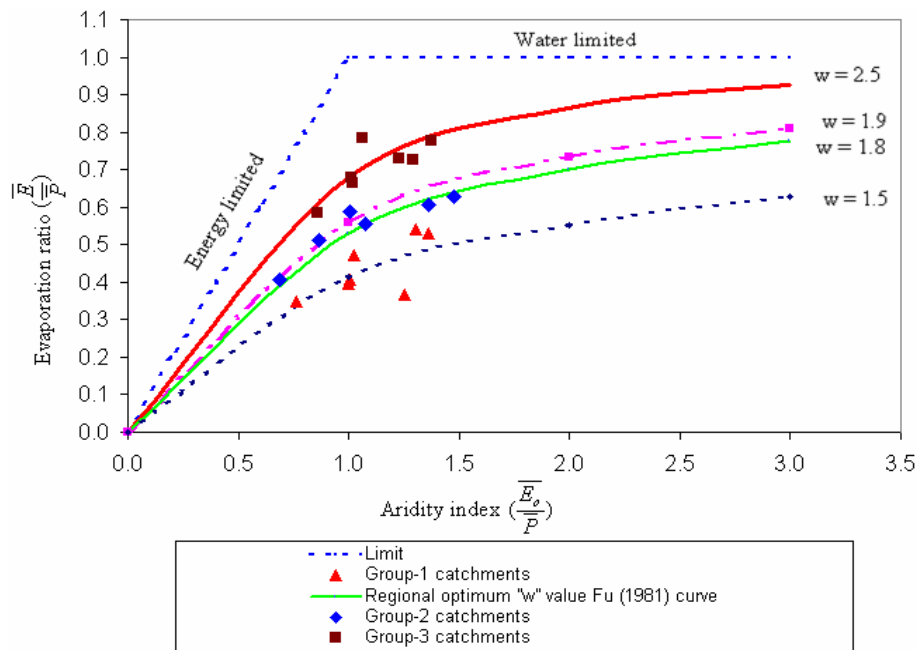
Fig. 4. Mean annual evaporation ratio ($\frac{\overline{E}}{P}$) as a function of Aridity Index ($\frac{\overline{E_0}}{P}$) for different values of w using Fu (1981) curve.

Table 3. Average goodness-of-fit statistics Nash and Sutcliffe efficiency (E_{NS}) and root mean squared error (RMSE) for prediction of regional long term mean annual streamflow using Fu's curve.

	E_{NS} (−)	RMSE (mm yr^{-1})	Calibrated parameter "w"
All catchments	0.70	177.51	1.8
Group-1 catchments[1]	0.87	76.36	1.5
Group-2 catchments[2]	0.97	57.22	1.9
Group-3 catchments[3]	0.85	58.23	2.5

[1] Gilegl Abay, Koga, Gumera, Jedeb, Uke, Gilgel Beles and Beles.

[2] Fetam, Dura, Guder, Muger, Temcha and Megech.

[3] Neshi, Chemoga, Birr, Rib, Robi Gumero, Robi Jida and Didessa.

catchments. The Nash and Sutcliffe efficiency (E_{NS}) and root mean squared error (RMSE) show that the long term average annual streamflow for each group of catchment was predicted adequately using Eq. (4).

From the results of modeled individual catchments, it is noted that the calibrated parameter w ranges between 1.4 and 3.6. This may suggest that the Upper Blue Nile catchments under consideration exhibit different catchment characteristics. Zhang et al. (2004) pointed out that smaller values of w are associated with high rainfall intensity, seasonality, steep slope and lower plant available soil water storage capacity. However, it is difficult to represent these characteristics explicitly in a simple model (Zhang et al., 2004;

Yang et al., 2007). Typically the result of the analysis from group-1 catchments in our study indicates that a larger fraction of precipitation becomes surface runoff, which results in lower evaporation ratios for this group compared to the other groups. Besides, the computed runoff coefficients for group-1 catchments ranges between 0.5–0.7 suggest that surface runoff was dominant in these catchments. The catchments in Group-2 have higher evaporation ratio and lower runoff coefficients (0.37–0.47) than Group-1. But Group-3 catchments have higher evaporation ratios, lower runoff potential and hence have lower values of the runoff coefficients (0.21–0.33).

It is also noted that the parameter w summarizes integrated catchment characteristics such as land cover, geology, soil properties and topography. It is not possible to fully explain the effects of w for each group of catchment due to the lack of detail data of physiographic characteristics in the region.

4.2 Modeling streamflow at monthly time scale

Modeling at finer time scale (monthly and daily) requires the inclusion of soil moisture dynamics to accurately estimate the water balance. In a top down modeling approach, model complexity has to be increased when deficiencies of the model structure in representing the catchment behavior is encountered (Jothityangkoon et al., 2001; Atkinson et al., 2002; Montanari et al., 2006; Zhang et al., 2008). Therefore, a somewhat more complex model structure has been applied that is still very simple and has four parameters (see Fig. 3).
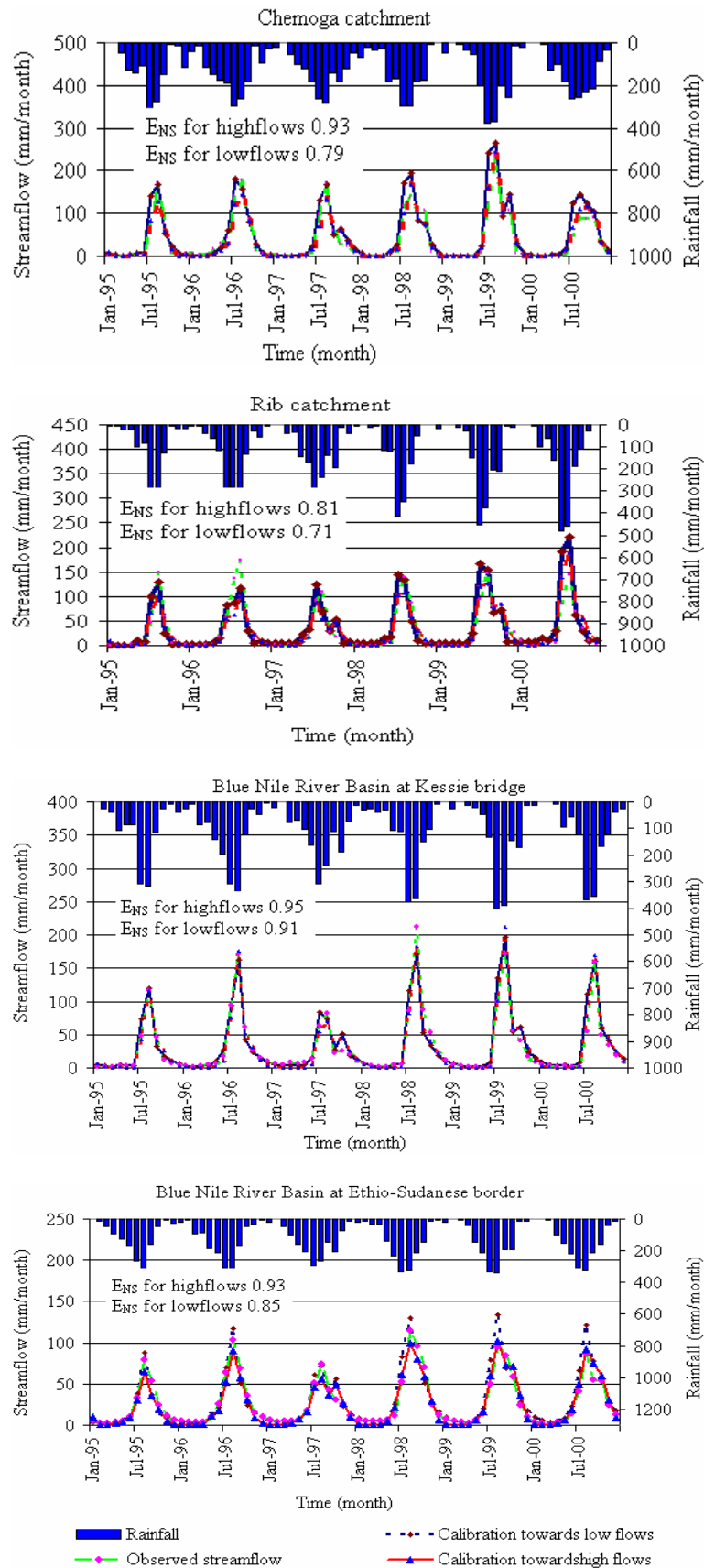
Fig. 5. Observed and simulated streamflows during calibration period (1995–2000) for selected catchments.
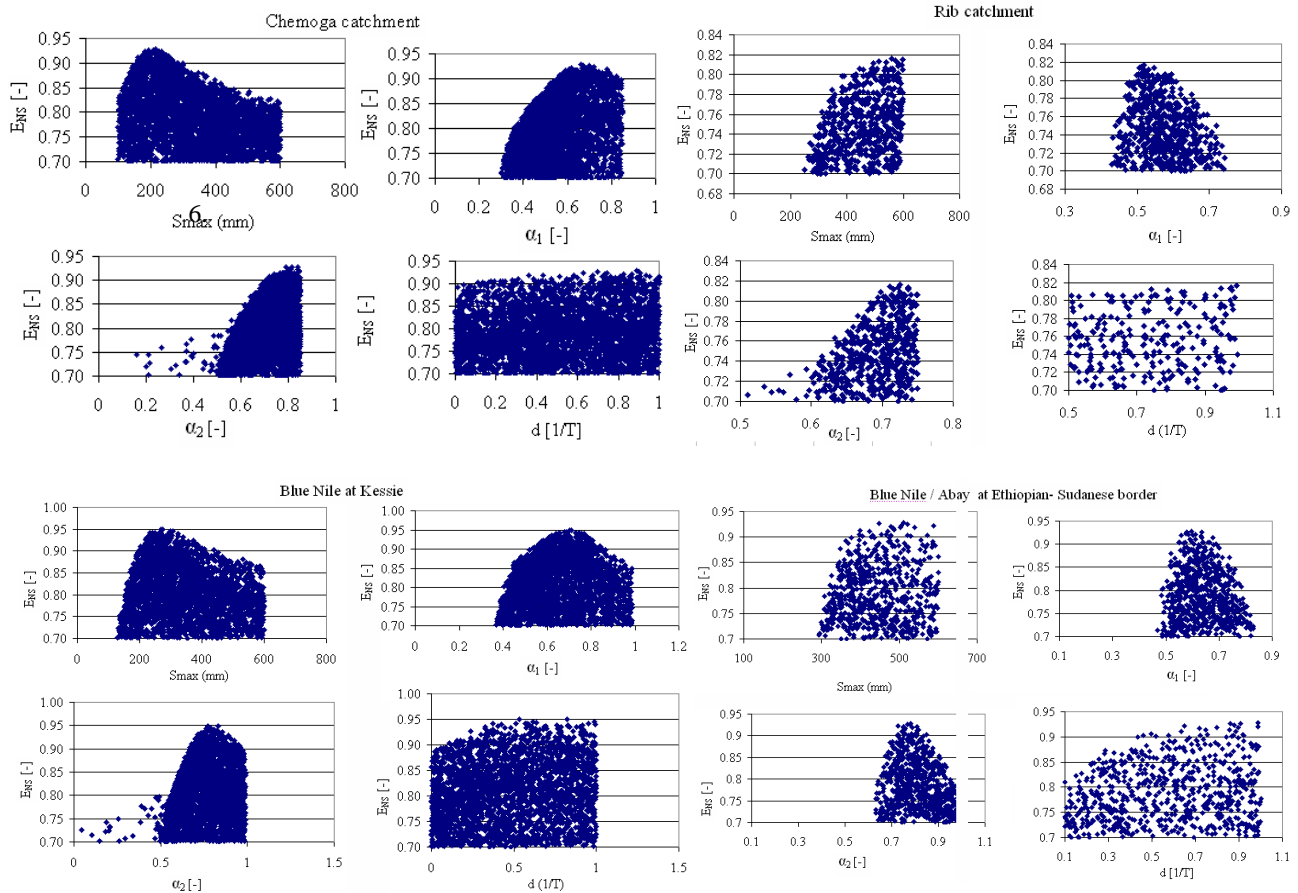
Fig. 6. GLUE dotty plots of selected meso-scale catchments and Blue Nile at larger scale at Kessie Bridge and Ethiopian-Sudanese border.

The monthly streamflows were calibrated for the period 1995–2000 and validated for the period 2001–2004. In the manual calibration and validation the Nash and Sutcliffe coefficient efficiency was used as leading performance measure. The main objective of calibration is finding the optimal parameter set that maximizes or minimizes the objective function for the intended purposes. In the parameter identification process, different parameter sets were sampled randomly from a priori feasible parameter space as shown in Table 4, which is in agreement with the literature (Zhang et al., 2008) and manual calibration in this study.

The dynamic water balance model was calibrated and validated for the twenty catchments and also at the two larger catchments with gauging stations at Kessie Bridge station ($64\,252\,\mathrm{km}^2$) and at the Ethiopian-Sudanese border ($173\,686\,\mathrm{km}^2$) to test the ability of the model at large spatial scale. During calibration Nash and Sutcliffe coefficients were obtained in the range of 0.52–0.95 (dominated by high flows) and 0.33–0.93 using logarithmic discharge values when calculating E_{NS} (dominated by low flows).

Similarly, during the validation period Nash and Sutcliffe efficiencies were obtained in the range of 0.55–0.95 during high flows and 0.12–0.91 during low flows. The model

Table 4. Ranges of parameter values for the catchments modeled in the Upper Blue Nile basin based on manual calibration and Zhang et al. (2008).

Catchment	Lower/upper bound			
	S_{max} [mm]	α_1 [−]	α_2 [−]	d [1/month]
Gilgel Abay, Koga, Birr, Fetam, Neshi	100–600	0–1	0–1	0–1
Dura, Gilgel Beles, Gumera, Megech, Rib, Robigumero, Robijida, Didessa	100–600	0.1–0.75	0.1–0.75	0–1
Chemoga, Beles, Guder	100–600	0.1–0.85	0.1–0.85	0–1
Muger, Temcha, Uke, Jedeb	100–600	0–0.9	0–0.8	0–1

results reveal that during calibration, the model gave reasonable results in most of the catchments including the simulation at larger scale at Kessie Bridge station ($E_{\mathrm{NS}} = 0.95$) and at the Ethiopian-Sudanese border ($E_{\mathrm{NS}} = 0.93$). However, during the validation period in some catchments the

low flows were not captured well by the model. Though a lot of uncertainties in model structure and model parameters were common in hydrological models, it is speculated that the likely reason for poor efficiency values in some catchments were more related to the uncertainties in the input data sets. Figure 5 shows observed and predicted streamflows using automatic calibration for selected meso-scale catchments and the larger scale results at Kessie Bridge station and Ethiopian-Sudanese border.

The optimal parameter values obtained using GLUE framework together with parameters obtained manually are presented in Table 5.

It is clearly demonstrated that the parameter values differ and the performance of the model improved using a GLUE framework. The parameter α_1 in majority of the catchments shows that the rainfall amount retained by the catchments is not significant, thus fast runoff generation process are dominant in the studied catchments. This high responsiveness is also in line with field observations where the formation of surface runoff (and significant soil erosion) can be observed. The values of evaporation efficiency parameter α_2 are higher in some catchments which implies higher partitioning of available water into evaporation. The higher evaporation efficiency parameter in these catchments reveals that the catchments were relatively having high forest cover and evaporation was dominant and less surface runoff was generated in these catchments. The dotty plots used to map the parameter value and their objective function values as a means of assessing the identifiability of parameters are shown in Fig. 6.

It can be seen that most of the parameters in the Upper Blue Nile catchments are reasonably well identifiable; however, the recession constant d exhibit poor identifiability in the majority of the catchments. It is speculated that parameter uncertainty and model structural errors could be the reason for the poorly identifiable groundwater parameter.

Furthermore, the model performances in the objective function space of Pareto-optimal fronts resulting from the monthly water balance model were investigated (see Fig. 7).

From multi-objective optimization point of view, the Pareto-optimal solutions are all equally important to achieve a better model simulation. The Pareto based approach is also important to compare different model structures in such a way that model improvement can be attained as the Pareto-optimal front progressively moves towards the origin of the objective function space (Fenicia et al., 2007; Wang et al., 2007). From Fig. 7 it can be noticed that for different catchments the Pareto-optimal set of solutions approach to the origin differently. It is demonstrated that the model structure performs better at the larger scale than for the meso-scale catchments. As the objective function values get closer to the origin, the chosen model structure represents the hydrologic system better.
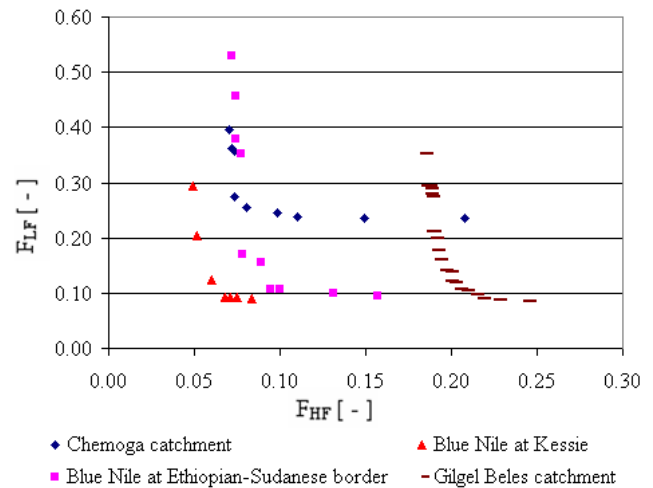
Fig. 7. Pareto-optimal fronts of parameter sets at different meso-scale catchments and Blue Nile at the larger scale based on the selected objective functions [low flows (F_{LF}), high flows (F_{HF})].

5 Conclusions

The Upper Blue Nile catchment water balance has been analyzed at different temporal and spatial scales using Budyko's framework. The analysis included water balance at mean annual, annual and monthly time scales for meso to large scale catchments. A Budyko-type curve (Fu, 1981) was applied to explore the first order control based on available water and energy over mean annual and annual time scales. The results demonstrated that predictions are not good in the majority of the catchments at annual time scale. This implies that at annual scale the water balance is not dominated only by precipitation and potential evaporation. Thus, increased model complexity to monthly time scale is necessary for a realistic simulation of the catchment water balance by including the effects of soil moisture dynamics. Parameters were identified using the Generalized Likelihood Uncertainty Estimation (GLUE) framework in addition to manual calibration and the results showed that most of the parameters are identifiable and the model is capable of simulating the observed streamflow quite well. The applicability of this model was tested earlier in 250 catchments in Australia with different rainfall regimes across different geographical regions and results were encouraging (Zhang et al., 2008; Fang et al., 2009). Similarly, in the Upper Blue Nile case, the model performs well in simulating the monthly streamflow of the twenty investigated catchments.

With only four parameters the simple model has the advantage of minimal equifinality. Despite the uncertainties in input data, parameters and model structure, the model gives reasonable results for the Upper Blue Nile catchments. However, it is suggested that on annual time scale the reasons for poor model efficiencies in majority of the catchments, which followed distinct Budyko-type curves, needs further research. It is recommended that future work should focus

Table 5. Comparison of automatic (GLUE) single objective and manually calibrated parameters and E_{NS} values of the twenty selected Upper Blue Nile catchments during the period 1995–2000.

Catchment	Optimized parameters (GLUE)					Manually calibrated parameters				
	S_{max} [mm]	α_1 [−]	α_2 [−]	d [1/month]	E_{NS} [−]	S_{max} [mm]	α_1 [−]	α_2 [−]	d [1/month]	E_{NS} [−]
Beles	538.09	0.46	0.53	0.96	0.71	365.00	0.50	0.52	0.85	0.70
Birr	253.62	0.76	0.92	0.87	0.93	330.00	0.57	0.62	0.91	0.82
Chemoga	216.40	0.66	0.81	0.89	0.93	260.00	0.60	0.63	0.90	0.90
Didessa	590.02	0.58	0.85	0.48	0.52	520.00	0.64	0.86	0.23	0.52
Dura	331.56	0.65	0.63	0.94	0.92	360.00	0.63	0.60	0.86	0.91
Fetam	420.89	0.56	0.50	0.99	0.89	280.00	0.52	0.67	0.35	0.81
Gilgel Abay	349.30	0.71	0.88	0.12	0.82	390.00	0.60	0.86	0.60	0.81
Gilgel Beles	280.03	0.57	0.35	0.98	0.91	280.00	0.55	0.47	0.90	0.89
Guder	306.01	0.83	0.45	0.94	0.72	390.00	0.67	0.41	0.85	0.71
Gumera	230.82	0.68	0.39	1.00	0.73	350.00	0.47	0.41	0.89	0.72
Jedeb	315.96	0.58	0.43	0.93	0.79	260.00	0.58	0.41	0.75	0.78
Koga	200.14	0.64	0.46	0.51	0.79	240.00	0.60	0.48	0.60	0.79
Megech	313.58	0.55	0.61	0.98	0.81	390.00	0.55	0.62	0.78	0.78
Muger	190.52	0.79	0.60	0.97	0.88	210.00	0.63	0.60	0.85	0.84
Neshi	397.90	0.79	0.82	0.93	0.80	380.00	0.66	0.64	0.75	0.75
Rib	558.43	0.52	0.72	0.99	0.82	370.00	0.63	0.73	0.60	0.76
Robigumero	512.88	0.53	0.73	0.02	0.74	500.00	0.50	0.75	0.65	0.73
Robijida	243.61	0.69	0.75	0.02	0.91	420.00	0.52	0.78	0.90	0.86
Temcha	190.80	0.66	0.63	0.99	0.83	200.00	0.62	0.60	0.80	0.82
Uke	441.60	0.70	0.33	0.74	0.82	430.00	0.67	0.33	0.70	0.82
Blue Nile at Kessie Bridge	268.25	0.70	0.77	0.53	0.95					
Upper Blue Nile at the border to Sudan	439.37	0.76	0.74	0.39	0.93					

on the regionalization of the optimal parameter sets from the monthly model presented in this paper for prediction of streamflow in ungauged catchments in the Upper Blue Nile basin.

Appendix A

Details of equation used in the model structure

Figure 3 illustrates the model structure of the dynamic monthly water balance model. Rainfall $P(t)$ at time step t partitions into direct runoff $Q_d(t)$ and $X(t)$. $X(t)$ is a lumped water balance component known as catchment rainfall retention which consists of the amount of retained water for catchment water storage dS/dt, $E(t)$ and recharge $R(t)$.

$$P(t) = Q_d(t) + X(t) \qquad (A1)$$

where $P(t)$, and $Q_d(t)$ are monthly rainfall and direct runoff, respectively. The units of all fluxes are mm month^{-1}.

Analogous to Budyko's hypothesis, Zhang et al. (2008) defined the demand limit for $X(t)$ to be the sum of dS/dt and potential evaporation (E_0), which is termed as $X_0(t)$ and the supply limit as $P(t)$. If the sum of available storage capacity and potential evaporation is very large as compared

to the supply, then $X(t)$ approaches $P(t)$ whereas if the sum of available storage capacity and potential evaporation is smaller than the supply, $X(t)$ approaches $X_0(t)$. This postulate can be written as:

$$\frac{X(t)}{P(t)} \to 1, \text{ as } \frac{X_0(t)}{P(t)} \to \infty \text{ for very dry conditions} \quad (A2)$$

$$X(t) \to X_0(t), \text{ as } \frac{X_0(t)}{P(t)} \to 0 \text{ for very wet conditions} \quad (A3)$$

The catchment rainfall retention can be expressed as:

$$X(t) = \begin{cases} P(t)\, F\left[\left(\frac{X_0(t)}{P(t)}\right), \alpha_1\right], & P(t) \neq 0 \\ 0, & P(t) = 0 \end{cases} \quad (A4)$$

where F [−] is the Fu-curve Eq. (4) and α_1 is the retention efficiency, whereby larger α_1 values result in more rainfall retention and less direct runoff.

From Eqs. (A1) and (A4) the direct runoff is calculated as:

$$Q_d = P(t) - X(t) \qquad (A5)$$

The water availability $W(t)$ for partitioning can be computed as:

$$W(t) = E(t) + S(t) + R(t) \qquad (A6)$$

Sankarasubramania and Vogel (2002) defined the evaporation opportunity as maximum water that can leave the basin as evaporation at any given time t.

$$Y(t) = E(t) + S(t) \tag{A7}$$

For the partition of available water, the demand limit for $Y(t)$ is the sum of the soil water storage capacity (S_{max}) and potential evaporation $E_0(t)$ termed as $Y_0(t)$, while the supply limit is the available water $W(t)$. Analogous to Budyko's hypothesis, Zhang et al. (2008) postulated that:

$$\frac{Y(t)}{W(t)} \to 1 \text{ as } \frac{Y_0(t)}{W(t)} \to \infty, \text{ for dry conditions,} \tag{A8}$$

and

$$Y(t) \to Y_0(t) \text{ as } \frac{Y_0(t)}{W(t)} \to 0, \text{ for wet conditions.} \tag{A9}$$

The evaporation opportunity can be computed as:

$$Y(t) = \begin{cases} W(t) \, f \left[\frac{E_0(t)}{W(t)}, \alpha_2 \right], & W(t) \neq 0 \\ 0, & W(t) = 0 \end{cases} \tag{A10}$$

From Eqs. (A6) and (A10) the groundwater recharge $R(t)$ can be estimated as:

$$R(t) = W(t) - Y(t) \tag{A11}$$

To estimate the evaporation, the demand limit is $E_0(t)$ and the supply limit is $W(t)$, then $E(t)$ can be computed as:

$$E(t) = \begin{cases} W(t) \, F \left[\frac{E_0(t)}{W(t)}, \alpha_2 \right] & W(t) \neq 0 \\ 0, & W(t) = 0 \end{cases} \tag{A12}$$

where α_2 is a model parameter representing the evaporation efficiency. Equation (A12) is similar with Eq. (4) with the exception that precipitation is replaced by water availability $W(t)$ to take into account the effect of catchment water storage.

Zhang et al. (2008) also emphasized that Eqs. (A10) and (A12) use the same parameter. This is due to the fact that the groundwater recharge is essentially determined from evaporation efficiency. As evaporation efficiency becomes larger, i.e. for large values of α_2, the recharge is diminished. Using Eqs. (A10) and (A12), the soil water storage can be computed as:

$$S(t) = Y(t) - E(t) \tag{A13}$$

The groundwater storage is treated as linear reservoir. Thus, the base flow $Q_b(t)$ and the groundwater storage $G(t)$ can be modeled as:

$$Q_b(t) = d \, G \, (t - 1) \tag{A14}$$

$$G(t) = (1 - d \, \Delta t) \, G \, (t - 1) + R \, \Delta t \tag{A15}$$

where Q_b, G, and d are the baseflow [mm month^{-1}], groundwater storage [mm], and reservoir constant [1/month], respectively.

References

Abdo, K. S., Fisha, B. M., Rientjes, T. H. M., and Gieske, A. S. M.: Assessment of climate change impacts on the hydrology of Gilgel Abay catchment in Lake Tana basin, Ethiopia, Hydrol. Process., 23, 3661–3669, doi:10.1002/hyp.7363, 2009.

Abtew, W., Melesse, A. M., and Dessalegne, T.: Spatial, inter and intra-annual variability of the Upper Blue Nile Basin rainfall, Hydrol. Process., 23, 3075–3082, doi:10.1002/hyp.7419, 2009.

Allen, R. G., Pereira, L. S., Raes, D., and Smith, M.: Crop Evapotranpiration: Guildlines for computing crop water requirements, FAO Irrigation and Drainage Paper No. 56, Food and Agriculture Organization, Land and Water, Rome, Italy, 1998.

Atkinson, S., Woods, R. A., and Sivapalan, M.: Climate and landscape controls on water balance model complexity over changing time scales, Water Resour. Res., 38(12), 1314, doi:10.1029/2002WR001487, 2002.

BCEOM.: Abay Basin Integrated master plan study, main report Ministry of water resources, Addis Ababa, Phase two, Volume three Agriculture, 1–2, 1999.

Beven, K. and Binley, A.: The future of distributed models: Model calibration and uncertainty prediction, Hydrol. Process., 6, 279–298, 1992.

Budyko, M. I.: Climate and life, Academic, New York, 1974.

Camberlin, P.: Rainfall anomalies in the Source Region of the Nile and their connection with the Indian Summer Monsoon, J. Climate, 1380–1392, 1997.

Conway, D.: Water balance model of the Upper Blue Nile in Ethiopia, Hydrolog. Sci. J., 42, 265–286, 1997.

Conway, D.: Climate and Hydrology of the upper Blue Nile River Basin, Geogr. J., 166(1), 49–62, 2000.

Conway, D.: From head water tributaries to international river: Observing and adapting to climate variability and change in the Nile Basin, Global Environ. Change, 15, 99–114, 2005.

Donohue, R. J., Roderick, M. L., and McVicar, T. R.: On the importance of including vegetation dynamics in Budyko's hydrological model, Hydrol. Earth Syst. Sci., 11, 983–995, doi:10.5194/hess-11-983-2007, 2007.

ENTRO.: Cooperative regional assessment for watershed management Transboundary Analysis Abay-Blue Nile sub-Basin, The Nile Technical Regional office (ENTRO), Addis Ababa, Ethiopia, 2007.

Fang, Z., Zhang, L., and Xu, Z.: Effects of vegetation cover change on stream flow at a range of spatial scales, 18th World IMACS/MODSIM Congress cairns Australia, 13–17 July, 2009.

Fenicia, F., Savenije, H. H. G., Matgen, P., and Pfister, L.: A comparison of alternative multi objective calibration strategies for hydrological modeling, Water Res., 43, 3434, doi:10.1029/2006WR005098, 2007.

Fu, B. P.: On the calculation of the evaporation from land surface, Sci. Atmos. Sin., 5(1), 23–31, 1981.

Gebreyohannis, S. G., Taye, A., and Bishop, K.: Forest cover and stream flow in a headwater of the Blue Nile: complementing observational data analysis with community perception, Ambio, 39, 284–294, doi:10.1007/s13280-010-0047-y, 2010.

Gerrits, A. M. J., Savenije, H. H. G., Veling, E. J. M., and Pfister, L.: Analytical derivation of the Budyko Curve based on rainfall characterstics and a simple evaporation model, Water Resour. Res., 45, W04403, doi:10.1029/2008WR007308, 2009.

Gupta, H. V., Sorooshian, S., and Yapo, P. O.: Toward improved calibration of hydrologic models: Multiple and non-commensurable measures of information, Water Resour. Res., 34(4), 751–764, 1998.

Haile, A. T., Rientjes, T. H., Gieske, M., and GebreMichael, M.: Rainfall variability over mountainous and adjacent Lake areas: the case of Lake Tana basin at the source of the Blue Nile River, J. Appl. Meteorol. Clim., 48, 1696–1717, 2009.

Hargreaves, G. H. and Allen, R. G.: History and Evaluation of Hargreaves Evapotranspiration Equation, J. Irrig. Drain. Eng.-ASCE, 129(1), 53–63, 2003.

Hargreaves, G. H. and Samani, Z. A.: Estimating potential evaporation. J. Irrig. Drain. Eng.-ASCE, 108(3), 225–230, 1982.

Johnson, P. A. and Curtis, P. D.: Water Balance of Blue Nile River Basin in Ethiopia, J. Irrig. Drain. Eng.-ASCE, 120(3), 573–590, 1994.

Jothityangkoon, C., Sivapalan, M., and Farmer, D. L.: Process control of water balance variability in a large semi-arid catchment down ward approach to hydrological model development, J. Hydrol., 254(1–4), 174–198, 2001.

Kebede, S., Travi, Y., Alemayehu, T., and Marc, V.: Water balance of Lake Tana and its sensitivity to fluctuations in rainfall, Blue Nile basin, Ethiopia, J. Hydrol., 316, 233–247, 2006.

Koster, R. D. and Suarez, M. J.: A simple frame work for examining the inter annual variability land surface moisture fluxes, J. Climate, 12, 1911–1917. 1999.

Legates, D. R. and McCabe, G. J.: Evaluating the use of "goodness-of- fit" measures in hydrologic and hydroclimatic model validation, Water Resour. Res., 35, 233–241, 1999.

Milly, P. C. D.: Climate, Soil water storage, and the average annual water balance, Water Resour. Res., 30(7), 2143–2156, 1994.

Mishra, A. and Hata, T.: A Grid based runoff generation and flow routing model for the upper Blue Nile Basin, Hydrolog. Sci. J., 51(2), 191–205, 2006.

Montanari, L., Sivapalan, M., and Montanari, A.: Investigation of dominant hydrological processes in a tropical catchment in a monsoonal climate via the downward approach, Hydrol. Earth Syst. Sci., 10, 769–782, doi:10.5194/hess-10-769-2006, 2006.

Ol'dekop, E. M.: On evaporation from the surface of river basins, Transactions on Meteorological Observations, Lur-evskogo, Univ. of Tartu, Tartu, Estonia, 1911.

Pike, J. G.: The estimation of annual runoff from meteorological data in a tropical climate, J. Hydrol., 2, 116–123, 1964.

Potter, N. J., Zhang, L., Milly, P. C. D., McMahon, T. A., and Jakeman, A. J.: Effects of rainfall seasonality and soil moisture capacity on mean annual water balance for Australian catchments, Water Resour. Res., 41, W06007, doi:10.1029/2004WR003697, 2005.

Potter, N. J. and Zhang, L.: Inter annual variability of catchment water balance in Australia, J. Hydrol., 369, 120-129, 2009.

Sankarasubramania, A. and Vogel, R. M.: Annaual Hydroclimatology of United States, Water Resour. Res., 38(6), 1083, doi:10.1029/2001WR000619, 2002.

Sankarasubramania, A. and Vogel, R. M.: Hydroclimatology of the contential United States, Geophys. Res. Lett., 30, 1363, doi:10.1029/2002GL015937, 2003.

Schreiber, P.: Über die Beziehungen zwischen dem Niederschlag und der Wasserführung der Flüsse in Mitteleuropa, Meteorol. Z., 21, 441–452, 1904.

Seleshi, Y. and Zanke, U.: Recent change in rainfall and rainy days in Ethiopia. International Journal of climatology, Int. J. Climatol., 24, 973–983, doi:10.1002/joc.1052, 2004.

Setegne, S. G., Srinivasan, R., and Dargahi, B.: Hydrological Modelling in the Lake Tana Basin, Ethiopia using SWAT model, Open Hydrol. J., 2, 24–40, 2008.

Setegne, S. G., Srinivasan, R., Melesse, A. M., and Dargahi, B.: SWAT model application and prediction uncertainty analysis in the Lake Tana Basin, Ethiopia, Hydrol. Process., 24, 357–367, 2010.

Steenhuis, T., Collick, A., Easton, Z., Leggesse, E., Bayabil, H., White, E., Awulachew, S., Adgo, E., and Ahmed, A.: Predicting discharge and sediment for the Abay (Blue Nile) with a simple model, Hydrol. Process., 23, 3728-3737, 2009.

Teferi, E., Uhlenbrook, S., Bewket, W., Wenninger, J., and Simane, B.: The use of remote sensing to quantify wetland loss in the Choke Mountain range, Upper Blue Nile basin, Ethiopia, Hydrol. Earth Syst. Sci., 14, 2415–2428, doi:10.5194/hess-14-2415-2010, 2010.

Turc, L.: Le bilan d'eau des sols Relation entre la precipitation l'evapporation et l'ecoulement, Ann. Agron., 5, 491–569, 1954.

Uhlenbrook, S., Seibert, J., Leibundgut, Ch., and Rodhe, A.: Prediction uncertainty of conceptual rainfall-runoff models caused by problems to identify model parameters and structure, Hydrolog. Sci. J., 44(5), 279–299, 1999.

Uhlenbrook, S., Mohamed, Y., and Gragne, A. S.: Analyzing catchment behavior through catchment modeling in the Gilgel Abay, Upper Blue Nile River Basin, Ethiopia, Hydrol. Earth Syst. Sci., 14, 2153–2165, doi:10.5194/hess-14-2153-2010, 2010.

UNESCO – United Nations, Educational, Scientific and Cultural Organization: National Water Development Report for Ethiopia, UN-WATER/WWAP/2006/7, World Water Assessment program, Report, MOWR, Addis Ababa, Ethiopia, 2004.

Wale, A., Rientjes, T. H. M., Gieske, A. S. M., and Getachew, H. A.: Ungauged catchment contributions to Lake Tana's water balance, Hydrol. Process., 23, 3682–3693, 2009.

Wang, Y., Dietrich, J., Voss, F., and Pahlow, M.: Identifying and reducing model structure uncertainty based on analysis of parameter interaction, Adv. Geosci., 11, 117–122, doi:10.5194/adgeo-11-117-2007, 2007.

Yang, D., Sun, F., Liu, Z., Cong, Z., Ni, G., and Lei, Z.: Analyzing spatial and temporal variability of annual water-energy balance in nonhumid regions of China using the Budyko hypothesis, Water Resour. Res., 43, W04426, doi:10.1029/2006WR005224, 2007.

Yang, D., Shao, W., Yeh, P. J. F., Yang, H., Kanae, S., and Oki, T.: Impact of vegetation coverage on regional water balance in the nonhumid regions of china, Water Resour. Res., 45, W00A14, doi:10.1029/2008WR006948, 2009.

Zhang, L., Dawes, W. R., and Walker, G. R.: Predicting the effect of vegetation changes on catchment average water balance, Tech. Rep.99/12 Coop. Res. Cent. Catch. Hydrol., Canbera, ACT, 1999.

Zhang, L., Dawes, W. R., and Walker, G. R.: Response of mean annual evapotranspiration to vegetation changes at catchment scale, Water Resour. Res., 37(3), 701–708, 2001.

Zhang, L., Hickel, K., Dawes, W. R., Chiew, F. H. S., and Western, A. W.: A rational function approach for estimating mean annual evapotranspiration, Water Resour. Res., 40, W02502, doi:10.1029/2003WR002710, 2004.

Zhang, L., Potter, N., Hickel, K., Zhang, Y. Q., and Shao, Q. X.: Water balance modeling over variable time scales based on the Budyko framework-Model development and testing, J. Hydrol., 360, 117–131, 2008.

Zhao, C., Nan, Z., and Cheng, G.: Evaluating Methods of Estimating and Modelling Spatial Distribution of Evapotranspiration in the Middle Heihe River Basin, China, Am. J. Environ. Sci., 1(4), 278–285, 2005.